

This discussion paper is/has been under review for the journal The Cryosphere (TC).
Please refer to the corresponding final paper in TC if available.

High-resolution modelling of the seasonal evolution of surface water storage on the Greenland Ice Sheet

N. S. Arnold, A. F. Banwell, and I. C. Willis

Scott Polar Research Institute, University of Cambridge, Lensfield Road,
Cambridge CB2 1ER, UK

Received: 25 October 2013 – Accepted: 25 November 2013 – Published: 20 December 2013

Correspondence to: N. S. Arnold (nsa12@cam.ac.uk)

Published by Copernicus Publications on behalf of the European Geosciences Union.

TCD
7, 6143–6170, 2013

Greenland surface
water

N. S. Arnold et al.

Title Page	
Abstract	Introduction
Conclusions	References
Tables	Figures
◀	▶
◀	▶
Back	Close
Full Screen / Esc	

Printer-friendly Version
Interactive Discussion



Abstract

Seasonal meltwater lakes on the Greenland Ice Sheet form when surface runoff is temporarily trapped in surface topographic depressions. The development of such lakes affects both the surface energy balance and dynamics of the ice sheet. Although areal extents, depths, and lifespans of lakes can be inferred from satellite imagery, such observational studies have a limited temporal resolution. Here, we adopt a modelling-based strategy to estimate the seasonal evolution of surface water storage for the ~3600 km² Paakitsoq region of W. Greenland. We use a high-resolution time dependent surface mass balance model to calculate surface melt, a supraglacial water routing model to calculate lake filling and a prescribed water-volume based threshold to predict lake drainage events. The model shows good agreement between modelled lake locations and volumes and those observed in 9 Landsat 7 ETM+ images from 2001, 2002 and 2005. We use the model to investigate the lake water volume required to trigger drainage, and the impact that this threshold volume has on the proportion of meltwater that runs off the ice supraglacially, is stored in surface lakes, or enters the subglacial drainage system. Model performance is maximised with prescribed lake volume thresholds between 4000 and 7500 times the local ice thickness. For these thresholds, lakes transiently store < 40 % of meltwater at the beginning of the melt season, decreasing to ~ 5 to 10 % by the middle of the melt season. 40 to 50 % of meltwater runs off the ice surface directly, and the remainder enters the subglacial drainage system through moulins at the bottom of drained lakes.

1 Introduction

The formation of surface meltwater lakes on the surface of the Greenland Ice Sheet (GrIS) (and other Arctic ice masses) during the melt season is a widely observed phenomenon. However, many of the lakes observed early in the melt season have disappeared or decreased in size by later in the summer (McMillan et al., 2007; Selmes

[Title Page](#)[Abstract](#)[Introduction](#)[Conclusions](#)[References](#)[Tables](#)[Figures](#)[◀](#)[▶](#)[Back](#)[Close](#)[Full Screen / Esc](#)[Printer-friendly Version](#)[Interactive Discussion](#)

et al., 2011; Liang et al., 2012; Fitzpatrick et al., 2013; Morriss et al., 2013). Whilst some lakes drain slowly by overflowing the lowest part of the lake rim, allowing water to escape from the depression by surface channel incision, other lakes drain rapidly by water-driven fracture propagation (i.e. “hydrofracture”) (Van der Veen, 2007; Das et al., 5 2008; Doyle et al., 2012; Tedesco et al., 2013). The sudden injection of large quantities of surface meltwater to the ice sheet bed and the associated reduction in basal friction has been proposed as a mechanism to explain observations of short-term increases in summer ice velocities following such drainage events (Zwally et al., 2002; Hoffman et al., 2011; Banwell et al., 2013). The storage (and subsequent release) of meltwater in 10 supraglacial lakes is a key control in determining both the timing, and rate of delivery, of water to the subglacial drainage system. This is important as it is widely accepted that the variability in magnitude and timing of meltwater input to the subglacial drainage system has a greater influence on subglacial water pressures, and thus ice motion, than simply the total volume of water input (Schoof, 2010; Bartholomew et al., 2011b, 15 2012; Colgan et al., 2011). However, despite numerous studies which compare ice velocity data to lake drainage observations from satellite imagery (e.g., Bartholomew et al., 2010, 2011; 2012; Hoffman et al., 2011; Sole et al., 2011, 2013; Sundal et al., 2011; Cowton et al., 2013; Joughin et al., 2013), there is still uncertainty about how supraglacial lake drainage events affect basal water pressures, uplift and ice velocity 20 over seasonal and annual time scales. Accurate estimates of potential water storage and the seasonal evolution of surface lake volumes on the GrIS will be an important component of ongoing work to understand how the ice sheet will respond to future climate scenarios.

2 Methods

25 Most studies of lake extent and dynamics have been based on a combination of direct surface observation and/or the use of multi-spectral satellite imagery (e.g., Box and Ski, 2007; Sneed and Hamilton, 2007; Sundal et al., 2009; Selmes et al., 2011; Liang

[Title Page](#)[Abstract](#)[Introduction](#)[Conclusions](#)[References](#)[Tables](#)[Figures](#)[|◀](#)[▶|](#)[◀](#)[▶](#)[Back](#)[Close](#)[Full Screen / Esc](#)[Printer-friendly Version](#)[Interactive Discussion](#)

et al., 2012). Whilst such studies have allowed the extent, and to a more limited degree, the evolution, of surface lakes to be ascertained for the times when such imagery is available, they are limited by the fact that lakes are transient features; not all lakes will be observed on any given image, and an image may not capture the maximum extent of any given lake. Recent studies using automated detection algorithms (e.g., Liang et al., 2012; Fitzpatrick et al., 2013; Morriss et al., 2013) have alleviated these problems somewhat, but still suffer to some extent from the availability of imagery of sufficient quality, and are perhaps best suited to tracking changes in total lake area over wide regions, rather than tracking the behaviour of individual lakes. High temporal resolution imagery is also only available at lower spatial resolution, meaning that smaller lakes are harder to identify.

In order to address these limitations, we follow Banwell et al. (2012b) and subsequently Banwell et al. (2013), in linking a high-resolution surface mass balance (SMB) model (originally developed for Arctic glaciers (Rye et al., 2010), and subsequently used to calculate melt over the Paakitsoq region of the GrIS (Banwell et al., 2012a)), to a new high-resolution Surface Routing and Lake Filling (SRLF) model in order to calculate the filling rates of surface lakes over the course of a melt season. This in turn is linked to a water volume threshold-based model of surface lake drainage (SLD) (Clason et al., 2012; Banwell et al., 2013).

In this study, we run the combined glaciohydrological model (which we call “G-Hyd”) for a $\sim 3600 \text{ km}^2$ area of the Paakitsoq region of W. Greenland, just north of Jacobshavn Isbrae (Fig. 1). Our primary aims are three-fold; first, to evaluate the model performance over a larger area of the ice sheet than that assessed by Banwell et al. (2012b); second, to investigate the impact of altering the water volume threshold for lake drainage on model performance and the behaviour of the supraglacial hydrological system; and third, to consider the possible implications of the modelled behaviour on the subglacial hydrology of the ice sheet.

Greenland surface water

N. S. Arnold et al.

[Title Page](#)

[Abstract](#)

[Introduction](#)

[Conclusions](#)

[References](#)

[Tables](#)

[Figures](#)

[|◀](#)

[▶|](#)

[◀](#)

[▶](#)

[Back](#)

[Close](#)

[Full Screen / Esc](#)

[Printer-friendly Version](#)

[Interactive Discussion](#)



2.1 The G-Hyd model

The SMB model consists of three coupled components: (i) an energy balance component that calculates the energy exchange between the glacier surface and the atmosphere using measured meteorological variables; (ii) an accumulation routine to calculate winter accumulation, and possible summer snowfall; and (iii) a subsurface component, simulating changes in temperature, density and water content in the snow, firn and upper ice layers, and hence refreezing and net runoff of water (Rye et al., 2010; Banwell et al., 2012a).

The SMB model is forced by meteorological variables from the JAR1 GC-Net station, 10 supplemented by data from the Swiss Camp GC-Net Station when JAR1 data were unavailable (Fig. 1) (Steffen and Box, 2001; Banwell et al., 2012a). The main forcing variables are the incoming global shortwave radiation, air temperature, relative humidity, and wind speed at a height of 2 m above the ice surface. Incoming longwave radiation data were not available for the Paakitsoq region, so these data were calculated using parameterizations (Banwell et al., 2012a, following Konzelmann et al., 1994). The 15 accumulation routine uses measured hourly precipitation from the ASAIIQ Greenland Survey station 437, ~4 km west of the ice margin at an elevation of 190 m a.s.l. (Fig. 1). This is distributed over the ice sheet using an elevation-dependent precipitation gradient. Snowfall is calculated from this and a threshold temperature for snowfall of 2 °C (Rye et al., 2010; Banwell et al., 2012a).

The SRLF model links a new algorithm, for calculating flow accumulation (upstream area) values over a digital elevation model (DEM) (Arnold, 2010), with a supraglacial water flow algorithm previously used on valley glaciers (Arnold et al., 1998) to calculate input hydrographs for all the depressions (and hence potential lakes) in the DEM. 25 The model uses the DEM to calculate lake hypsometry, which, together with the input hydrographs, allows lake depth and areal extent at any given time to be calculated. If a lake fills to its maximum extent, any further water inputs overflow into the downstream catchment. In this way, water can flow from its source on the ice sheet in a series of

TCD

7, 6143–6170, 2013

Greenland surface
water

N. S. Arnold et al.

Title Page	
Abstract	Introduction
Conclusions	References
Tables	Figures
◀	▶
◀	▶
Back	Close
Full Screen / Esc	
Printer-friendly Version	
Interactive Discussion	





“cascades” through multiple full lakes. This combined approach has been used by Banswell et al. (2012b) to model measured water volumes in an instrumented lake within a 100 km² area of the Paakitsoq region in 2011 with a high degree of accuracy.

The SLD model uses a water-volume based threshold to trigger lake drainage events.

- Fracture propagation and consequent lake drainage is assumed to occur if a lake reaches the volume needed to fill an inferred fracture extending from the ice surface to the bed (Clason et al., 2010; Banwell et al., 2013). The inferred width and length (i.e. the surface area) of the fracture can be varied in the model; we explore the model behaviour for inferred fracture areas (F_a) from 500 m^2 to $10\,000\text{ m}^2$, and also with an infinite volume threshold, which prevents lake drainage events. If a lake reaches the volume threshold for drainage (controlled by the inferred fracture area, and the ice thickness beneath the deepest part of the lake), the lake empties, and any further water inputs are assumed to enter the subglacial drainage system directly through a moulin at the lowest part of the depression which is assumed to stay open for the remainder of the melt season.

2.2 DEM processing

We use the GIMP product (Howat et al., 2012) for the high-resolution surface DEM required by our modelling strategy, at the posted 90 m spatial resolution. Initial inspection of the data showed too many small (often single DEM-celled) depressions within the DEM. To combat this, we smoothed the data with a 2×2 cell median filter to remove much of the noise, and then applied an 11 cell radius Gaussian filter to remove the “terracing” effect that is a consequence of the 1 m vertical resolution of the original data.

25 Ice thickness data are needed to calculate the lake drainage threshold volume for
each lake. We calculate ice thickness using the surface DEM and the 750 m resolution
bed DEM described in Plummer et al. (2008), resampled using bilinear interpolation to
90 m resolution.

2.3 Analysis of lakes observed in satellite imagery

The predicted lake areas and volumes are compared with observed lake areas and volumes derived from 9 Landsat 7 ETM+ images acquired in 2001 (7 July, 14 July, 1 August, and 8 August), 2002 (30 May, 17 June, 2 August and 3 September) and 2005 (16 June). Digital numbers were converted to reflectance values using standard methods (Chander et al., 2009). Following Box and Ski (2007), pixels with a Band 1 to Band 3 (blue to red) reflectance ratio above a certain threshold are considered to contain water. The threshold value used was chosen by comparing those pixels above the threshold by eye with true-colour projections of the imagery, in order to match as well as possible the apparent visible extent of water in the images, but to avoid as far as possible “false positive” identification of other blue pixels as containing water. Lakes are then identified as contiguous sets of water-containing pixels. The water depth in the pixels identified as containing water is then calculated using the method of Sneed and Hamilton (2007). This procedure uses the band 2 and band 4 reflectance data, but it also requires knowledge of the albedo of the bottom of each lake. We estimate the lake-bottom albedo on a lake-by-lake basis by creating a mask of each lake identified in the images, then dilating this mask by 1 pixel. The original lake mask is then removed, leaving a ring of pixels around the lake outline. The average reflectance of these pixels is assumed to be representative of the pixels within that lake. The volume of each lake is then calculated from the water depth of each pixel within the lake. For a fuller description of the application of the Box and Ski (2007) and Sneed and Hamilton (2007) method to the Paakitsoq region, refer to Banwell et al. (2014).

2.4 Model evaluation

We evaluate two aspects of model performance; the first focuses on the accuracy of the DEM in predicting potential lake locations; the second examines the predicted volumes of modelled lakes on the appropriate dates vs. volumes calculated from the satellite imagery.

TCD

7, 6143–6170, 2013

Greenland surface
water

N. S. Arnold et al.

[Title Page](#)

[Abstract](#)

[Introduction](#)

[Conclusions](#)

[References](#)

[Tables](#)

[Figures](#)

[◀](#)

[▶](#)

[Back](#)

[Close](#)

[Full Screen / Esc](#)

[Printer-friendly Version](#)

[Interactive Discussion](#)



- Assessing the agreement between observed lakes in the visible imagery and DEM depressions is difficult for several reasons. Conventional classification methods based on contingency tables are biased because there will be many more locations that do not contain lakes or depressions than those that do, and also because whilst a lake can only form in a depression, it is possible for a depression to exist in the DEM but for it not to contain an observed lake; insufficient water may have accumulated in the depression for it to be observed, or the lake may have drained. Thus, an apparent disagreement between visible imagery and the DEM need not be due to an error. Given this, we assess co-location between observed lakes and depressions within the DEM
- by calculating the centroid of each lake identified within the visible imagery, and then determining the numbers of lake centroids within depression boundaries identified in the processed DEM vs. the number of lake centroids outside depression boundaries. These values were converted into z scores by calculating the mean and standard deviation of the ratio for 1000 sets of the appropriate number of randomly distributed centroid locations within the study area.

We assess the modelled lake volumes by comparing them with the calculated observed lake volumes in the visible imagery at the appropriate dates using conventional regression techniques, and using the Nash–Sutcliffe model efficiency measure. In the former case, we also use the “weighted R^2 ” value (Krause et al., 2005), calculated as:

$$wR^2 = \begin{cases} |b| \cdot R^2 & \text{for } b \leq 1 \\ |b|^{-1} \cdot R^2 & \text{for } b > 1 \end{cases} \quad (1)$$

where b is the slope of the regression relationship. Weighting R^2 in this way quantifies over- or under-prediction by the model as well as the overall dynamics of model performance (Krause et al., 2005).

[Title Page](#)[Abstract](#)[Introduction](#)[Conclusions](#)[References](#)[Tables](#)[Figures](#)[|◀](#)[▶|](#)[◀](#)[▶](#)[Back](#)[Close](#)[Full Screen / Esc](#)[Printer-friendly Version](#)[Interactive Discussion](#)

3 Results

3.1 Modelled lake location

Overall agreement between observed lake locations in the Landsat imagery and depressions within the DEM is good, and is summarised in Table 1; depression outlines are also shown in Fig. 1 for visual comparison with the image obtained on 7 July 2001. The flow accumulation algorithm of the SLRF model (Arnold, 2010) identified 644 depressions within the DEM, ranging in size from 1 pixel (8100 m^2) to 791 pixels (6.4 km^2). Using a blue/red reflectance ratio threshold of 2, a total of 505 separate lakes were identified (taking account of lakes which appear in more than one image) in the satellite imagery, with a maximum size of 332 pixels (2.7 km^2), of which 252 had centroids located within depressions. Using a blue/red ratio threshold of 3, 229 lakes were identified, of which 179 had centroids within depressions. The largest lake for this threshold had an area of 277 pixels (2.2 km^2). As shown by the corresponding z scores for these numbers (Table 1), the chance of the coincidence in location between observed lakes and DEM depressions being due to random variation is vanishingly small.

3.2 Modelled lake volumes

Visual examination of the thresholded satellite imagery showed that a blue/red threshold of 2 tended to identify pale blue pixels some distance above the transient snowline as lakes. Sometimes these occurred in quasi-linear features that could perhaps be slush fields in shallow valleys on the ice surface; others, however, were isolated, very small clusters of pixels with no obvious topographic control. Thus, for the remainder of our analysis, we adopted a blue/red ratio threshold value of 3 to classify lake pixels, and from this determine water depths, and lake areas and volumes. Calculated water depth is not affected by this threshold value, however, and given that lower thresholds only increase the number of very shallow pixels around the edge of lakes (as well as the total number of apparently water-containing pixels with no obvious topographic con-

TCD

7, 6143–6170, 2013

Greenland surface
water

N. S. Arnold et al.

[Title Page](#)

[Abstract](#)

[Introduction](#)

[Conclusions](#)

[References](#)

[Tables](#)

[Figures](#)

[◀](#)

[▶](#)

[◀](#)

[▶](#)

[Back](#)

[Close](#)

[Full Screen / Esc](#)

[Printer-friendly Version](#)

[Interactive Discussion](#)



[Title Page](#)[Abstract](#)[Introduction](#)[Conclusions](#)[References](#)[Tables](#)[Figures](#)[|◀](#)[▶|](#)[◀](#)[▶](#)[Back](#)[Close](#)[Full Screen / Esc](#)[Printer-friendly Version](#)[Interactive Discussion](#)

trol, especially at higher elevations), calculated lake volume is also insensitive to this threshold.

Table 2 shows four measures of model performance as an estimator of observed lake volumes for the 9 images across the three years. 2001 and 2002, each with four images spanning early July to early August in 2001, and late May to early September in 2002, show similar results; the highest R^2 values occur for F_a values of 2500 m^2 to 4000 m^2 , but the regression slope shows the model generally under-predicts lake volume for these F_a values. As F_a increases, the R^2 decreases marginally, but the weighted R^2 value, and the Nash–Sutcliffe statistic all increase until an F_a of 7500 m^2 , after which they decrease again. The regression slope increases as F_a increases, however, reaching a maximum some way above 1 for an infinite volume threshold, which effectively prevents any drainage, and leads to modelled lakes greatly exceeding their observed volumes and a clear worsening of overall model performance. 2005, with just one image, from 16 June, shows different behaviour. Here, increasing F_a from 1000 m^2 to 2500 m^2 results in an improvement in model performance, but as F_a is increased more, there is no further change in model performance. Similar behaviour also occurs for the two early-season images in 2002; no significant change in model performance occurs for F_a higher than 2500 m^2 .

3.3 System behaviour for different drainage thresholds

Figure 2a shows the modelled evolution of total water storage in lakes in comparison with total modelled meltwater production for the three years, for $F_a = 5000\text{ m}^2$. The total volume of melt produced in the three years is quite similar ($3.6\text{--}3.8 \times 10^9\text{ m}^3$), but the seasonal evolution of melt is quite different. Melt begins earliest in 2005, stops, and then begins again, increasing rapidly to ~ 30 June, when a cool period slows down the rate of increase until around 20 July, when melt production increases again. 2002 shows a later, slower start in melt, but then a generally rapid rise in cumulative melt for much of the season, to reach the highest overall total of the three years. In 2001, melt

starts even later, and rises only slowly until around 10 June, when the rate begins to increase to a similar level to 2002 and 2005.

- Total lake volumes at the end of the melt season are also similar between the three years; around 5 % of the total melt produced is stored in lakes at the end of the season.
- 5 All three years show a peak in storage early in the season of around 35–40 % of melt, with an initial rapid fall in 2001 and 2002 to around 15 % by 30 May, followed by a slow decrease (but with considerable short-term variability) throughout the rest of the melt season. 2005 behaves differently; volume as a proportion of melt increases rapidly, but then decreases sharply once the short, early-season melt period finishes. Once melt
- 10 begins again around 18 May, lake volume as a proportion of overall melt increases until around 30 May, when it begins a similar downward trajectory to that observed in 2001 and 2002.

Figure 2b shows the cumulative lake volume, the cumulative volume of melt which runs off the ice sheet surface, and the cumulative volume of melt which enters the subglacial drainage system via moulin in drained lakes (all as proportions of total cumulative melt) for 2001 for F_a values of 1000 m^2 , 5000 m^2 and 10000 m^2 . Altering F_a has a large impact on the relative proportions of the melt which remains in storage on the ice, or which leaves the ice sheet supraglacially or subglacially. Very early in the melt season, all three F_a values exhibit similar behaviour; around 35 % of melt is stored in lakes, and around 60 % runs off the ice surface at the margin (the remainder is stored “in transit”, within slow flow within the snowpack).

For $F_a = 1000\text{ m}^2$, the first drainage events occur within ~3 days of the onset of melt (15 May), leading to a rapid increase in the proportion of melt entering the subglacial system to around 15 % by 18 May, which then rises increasingly slowly to around 30 % by 10 June. Direct supraglacial runoff remains at around 60 % of cumulative melt until this time. After 10 June, the proportion of melt flowing as subglacial runoff begins to increase, steadily at first but then at a decreasing rate, reaching a final value of around 62 % of melt. Supraglacial runoff as a proportion of total melt begins to decrease after 10 June, quickly at first but at a gradually declining rate, reaching final proportions

[Title Page](#)[Abstract](#)[Introduction](#)[Conclusions](#)[References](#)[Tables](#)[Figures](#)[|◀](#)[▶|](#)[◀](#)[▶](#)[Back](#)[Close](#)[Full Screen / Esc](#)[Printer-friendly Version](#)[Interactive Discussion](#)

Greenland surface water

N. S. Arnold et al.

[Title Page](#)[Abstract](#)[Introduction](#)[Conclusions](#)[References](#)[Tables](#)[Figures](#)[|◀](#)[▶|](#)[◀](#)[▶](#)[Back](#)[Close](#)[Full Screen / Esc](#)[Printer-friendly Version](#)[Interactive Discussion](#)

of ~35 % of melt. The proportion of water stored in supraglacial lakes decreases at a diminishing rate after the onset of drainage at around 18 May.

For F_a of 5000 m² and 10 000 m², the proportion of melt flowing off the ice sheet margin continues to rise until around 30 May and 9 June, reaching peak values of ~80 % and ~85 % respectively. Subglacial drainage begins on 23 May and 12 June respectively, leading to a decrease in the proportion of supraglacial runoff, and an increase in the proportion of melt entering the subglacial system. This increases steadily at first, and then at a decreasing rate, reaching end of summer values of ~40 % and ~28 % for 5000 m² and 10 000 m², respectively. Storage within lakes shows a general gradual decline, but with episodes when the proportion varies by 3–5 % over periods of a few days (particularly from ~10 June to ~20 July), with sudden drops which mark the drainage of individual large lakes. These individual drainage events are also visible in the time-series of subglacial water volume. Final stored proportions are ~5 %, and ~8 % of total melt. Total surface runoff decreases, reaching final values of ~54 % and ~62 %.

The upglacier progression of lake drainage events during 2001 for F_a values of 1000 m², 5000 m² and 10 000 m² is shown in Fig. 3a. Fewer events occur with higher F_a values, but in all three cases there is a very clear upglacier progression of lake drainage events. The gradient of the curves around which drainage events cluster is steeper for higher values of F_a ; the need for a higher volume of water leads to later lake drainage at any given elevation, as more time is needed for melt to accumulate in the lake basins. Interestingly, clear clustering of drainage events occurs; for $F_a = 1000\text{ m}^2$, there are two distinct clusters of events around 28/29 June, for lakes with elevations of 900–1000 m, and a second around 14 July at ~1100 m. Given the smaller total numbers of drainage events for higher F_a values, clustering is less apparent but there is still a cluster of drainage events around 2 July for $F_a = 5000\text{ m}^2$ for lakes with elevations around 950 m, and about 5 days later for $F_a = 10 000\text{ m}^2$. There is also a small cluster of events for $F_a = 5000\text{ m}$ around 24/25 July, at around 1100 m. Figure 4b shows the spatial distribution of lake drainage events for 2001 for $F_a = 5000\text{ m}^2$. Again, the

[Title Page](#)

[Abstract](#)

[Introduction](#)

[Conclusions](#)

[References](#)

[Tables](#)

[Figures](#)

[|◀](#)

[▶|](#)

[Back](#)

[Close](#)

[Full Screen / Esc](#)

[Printer-friendly Version](#)

[Interactive Discussion](#)



upglacier progression of drainage is very clear; three pairs of lakes within ~5 km of each other drain within 24 h of each other, and several other sets of neighbouring lakes drain within 2 days of each other (e.g. the pair of green lakes in the lower centre of the region, and three of the cluster of 5 yellow lakes just down-glacier from them).

- 5 Animations of the season-long filling and draining of surface lakes for 2001 for $F_a = 2500 \text{ m}^2$, 5000 m^2 and 7500 m^2 are available in the Supplement (Fig. S1a–c).

4 Discussion

There are three controls on the volume of any given lake; the size and shape of the depression on the ice surface in which it forms; the volume of meltwater which has flowed into the depression by a particular time, and whether a drainage event has occurred (which previous studies have shown maybe either complete or partial). Our finding of a significant coincidence in location between observed lakes and depressions in the DEM suggests that the DEM topography is accurate at the horizontal spatial scales used here, and also at vertical scales of 1–10 m. The good match between modelled and observed lake volumes also supports this. The fact that the model performance early in the melt season does not change with F_a values above 2500 m^2 suggests that the melt model is supplying accurate estimates of water inputs to the lakes, but that early in the melt season, the water volume drainage threshold plays little role in determining observed lake volumes as very few have collected sufficient meltwater to reach a drainage threshold; their volumes are effectively melt-limited. Later in the melt season, however, the drainage volume threshold plays an increasingly important role in determining which lakes drain, and when. Too low a threshold allows lakes to drain too quickly and at too small a volume; too large a threshold means lakes drain too late, and reach too high a volume. Our findings suggest that F_a values of around 4000 m^2 to 7500 m^2 times the local ice thickness produce the best match, although there is no particular value which emerges as the overall best-fit value, as the different measures of model performance suggest different optimum values. However, the fact that this be-

haviour occurs in both years with good seasonal image availability suggests the water volume drainage threshold effectively simulates at least some of the physical processes that control lake drainage events.

The temporal complexity of behaviour exhibited by the model (Figs. 2 and 3) results from the interaction between the upglacier progression of melt over the course of a melt season, the time taken for lakes to fill to the critical volume needed to trigger a drainage event (and the proportion of lakes which drain), and the distribution of lakes over the ice surface. Figure 4 shows the cumulative maximum water storage on the ice sheet surface with elevation. At lower elevations (below ~ 700 m), water storage is small; 5 lakes are relatively few in number, and small in volume. Between 700 m and ~ 1200 m, water storage increases markedly, with the impact of several very large lakes clearly visible. Above ~ 1200 m, the rate of storage increase with elevation declines, with the exception of one very large lake at ~ 1450 m.

Thus, very early in the melt-season, melt is confined to the lowest elevations on 15 the ice sheet, and runs off supraglacially. Lakes close to the margin begin to fill with water. They are relatively small, however, and even for low values of F_a , many do not drain; those which do reach their critical volume (and therefore drain) within a few days. Drainage of these lakes therefore begins to limit the total proportion of melt running off supraglacially for the runs with low F_a values; at higher F_a values, the these 20 lakes fill and then overtop their margins, allowing water to continue to flow downglacier supraglacially. For low F_a values, the proportion of water draining subglacially begins to increase early in the melt season, but at higher F_a values, water continues to accumulate on the surface, or simply runs off supraglacially.

As the season progresses, the proportion of melt water stored within lakes decreases, as total lake volume is limited by the size of the depressions themselves, 25 or by water entering the subglacial drainage system through drained lakes for low F_a value runs. At some point, however, drainage events begin to occur at higher values of F_a for the larger lakes found higher on the ice sheet. Thus, the proportion of subglacial runoff begins to increase in these runs; storage in lakes continues to decrease,

Title Page	
Abstract	Introduction
Conclusions	References
Tables	Figures
◀	▶
◀	▶
Back	Close
Full Screen / Esc	

[Printer-friendly Version](#)

[Interactive Discussion](#)



but with periods when storage increases as large lakes at higher elevations begin to fill, and with “step” decreases marking the drainage of these larger lakes at their volume thresholds. The proportion of melt flowing off supraglacially begins to decrease as more melt enters the subglacial system through lakes that have drained. The most active period of lake filling and draining occurs between around 10 June and the end of July; after this time, lake drainage events become fewer, but still occur into mid-August. Generally, most lakes which could drain (i.e. where the potential maximum water volume (determined by the topography) exceeds the volume threshold (determined by F_a and the local ice thickness)) have drained by the middle of August; water volumes in the lakes at higher elevations are limited by the small amounts of melt which occur at high elevation, so drainage events at higher elevations are rare.

The clear upglacier progression of lake drainage events (Fig. 3) is driven by two factors; the upglacier progression of melting at the onset of the melt season (linked to the general trend for lower melt at higher elevations), which leads to later and smaller inputs of water to lakes at higher elevations, and the overall trend for thicker ice in interior parts of the ice sheet, which leads to higher water volume thresholds for higher-elevation lakes. The clustering of lake drainage events is interesting, however. Fitzpatrick et al. (2013) have observed clustering of drainage events in the Russell Glacier region and argue that this suggests that some form of synoptic trigger mechanism, based on the seismic and velocity-response of the ice sheet to an “initial” event, could trigger additional, nearby drainage events, and that a lake-volume based drainage trigger seems unlikely. However, our model results suggest that a lake-volume threshold can lead to clustering of drainage events; lakes in a given area will receive broadly similar meltwater inputs (due to the relative spatial uniformity of melt across a relatively flat ice sheet surface with quite uniform albedo and surface energy flux at scales of ~ 1 km to ~ 10 km), and will also have broadly similar ice depths beneath them, and so will have similar volume thresholds for drainage. Lakes with unusually early (or late) drainage dates (given their elevation) occur where the local ice thickness is lower (or

Greenland surface water

N. S. Arnold et al.

[Title Page](#)

[Abstract](#)

[Introduction](#)

[Conclusions](#)

[References](#)

[Tables](#)

[Figures](#)

◀

▶

◀

▶

[Back](#)

[Close](#)

[Full Screen / Esc](#)

[Printer-friendly Version](#)

[Interactive Discussion](#)



higher) than the average for that elevation, or where the supraglacial catchment feeding the lake is unusually large (or small).

Of course, our results do not rule out the “triggering” of drainage events by other nearby events, but they show that clustering of drainage events does not rule out a volume-based trigger for the drainage of individual lakes either. In many ways, some combination of both effects would seem most likely; a lake would most probably need some threshold volume of water in order to create a hydrofracture to the bed, but the “moment” of drainage could be triggered by flexural stresses associated with a nearby drainage event once the lake was “primed” with sufficient water. The clear upglacier progression of drainage observed in all of the remote sensing-based studies, and the need for at least one lake in a region to drain “spontaneously” in order to trigger other drainage events, also seems to support some form of water volume threshold as a condition for lake drainage.

5 Conclusions

In this study, we have applied a linked surface mass balance/supraglacial water flow/lake drainage model to a 3600 km^2 region of the Greenland Ice Sheet. Our key findings are:

- The current generation of high resolution DEMs available for the Greenland Ice Sheet are sufficiently accurate to enable the prediction of potential supraglacial lake positions and extents.
- Our surface mass balance (SMB) model and surface routing and lake filling (SRLF) model is sufficiently accurate to provide realistic water inputs to lakes over a wider area of the ice sheet than has been investigated in previous studies (Banwell et al., 2012a, b, 2013a).
- When linked to a water volume threshold-based surface lake drainage (SLD) model, the combined glaciohydrological model (G-Hyd) is capable of producing

Title Page	
Abstract	Introduction
Conclusions	References
Tables	Figures
◀	▶
◀	▶
Back	Close
Full Screen / Esc	
Printer-friendly Version	
Interactive Discussion	



good agreement between modelled lake extents and observed lake extents from remotely-sensed imagery during three melt seasons (2001, 2005 and 2005).

- 5 – The model results suggest that the water volume threshold needed to trigger lake drainage is somewhat higher than that suggested or used by previous studies that have used volume-based thresholds (e.g., Clason et al., 2012; Banwell et al., 2013). We find the best model performance for inferred fracture areas of between approximately 4000 m² and 7500 m². However, no clear “best fit” value emerges, as different measures of model performance produce different optimal values.
- 10 – The overall pattern of behaviour produced by the model matches that observed in other observation-based studies. The model reproduces the overall upglacier trend in lake filling and drainage, and also exhibits spatial and temporal clustering of drainage events. Unlike the proposed synoptic triggering of Fitzpatrick et al. (2013), this clustering is found to be the result of nearby lakes experiencing similar filling rates, and having similar water volume thresholds due to similar ice thicknesses in the area of the lakes.
- 15 – The water volume threshold acts as a primary control on the overall proportion of melt which is stored on the ice surface vs. that which enters the subglacial drainage system. Low volume thresholds lead to smaller amounts of supraglacial storage, and larger amounts of melt entering the subglacial system compared with larger volume thresholds. For the best fit values of inferred fracture areas of between 4000 m² and 7500 m², lakes transiently store < 40 % of meltwater at the beginning of the melt season, but this decreases to ~ 5 to 10 % by the middle of the melt season. 40 to 50 % of meltwater runs off the ice surface directly, and 50 % to 40 % enters the subglacial drainage system through the bottom of drained lakes.

Numerous recent studies have highlighted the complexities in the relationship between supra- (and sub-) glacial hydrology, and surface velocity for areas of the Greenland Ice

TCD

7, 6143–6170, 2013

Greenland surface
water

N. S. Arnold et al.

[Title Page](#)

[Abstract](#)

[Introduction](#)

[Conclusions](#)

[References](#)

[Tables](#)

[Figures](#)

◀

▶

[Back](#)

[Close](#)

[Full Screen / Esc](#)

[Printer-friendly Version](#)

[Interactive Discussion](#)



Sheet (e.g. Bartholomew et al., 2010, 2011, 2012; Hoffman et al., 2011; Sole et al., 2011, 2013; Sundal et al., 2011; Cowton et al., 2013; Joughin et al., 2013). The recent study by Joughin et al. (2013) in particular highlights the fact that the timing of lake drainage events controls when much of the observed seasonal speedup occurs; they also argue that it is the combination of surface and bed slopes which act together to determine water flow directions, and the consequent patterns of velocity. The G-Hyd model reported here, used in conjunction with recent high quality, high spatial resolution surface topography data, is capable of predicting the locations, volumes and timings of water inputs to the subglacial drainage system with a good degree of accuracy. In future, models of this type will be able to provide the key surface water input estimates which will subsequently permit more effective modelling of the impact of subglacial hydrology on ice dynamics.

**Supplementary material related to this article is available online at
<http://www.the-cryosphere-discuss.net/7/6143/2013/tcd-7-6143-2013-supplement.zip>.**

15

Acknowledgements. This work was partially funded by the UK Natural Environment Research Council Doctoral Training grant to A. F. Banwell (LCAG/133) (CASE Studentship with The Geological Survey of Denmark and Greenland (GEUS)). We thank Andreas Ahlstrøm (GEUS), Douglas MacAyeal, and Marco Tedesco for valuable discussions throughout the research. We are also very grateful to Dorthe Petersen for proglacial discharge data from the ASIAQ Greenland Survey and to Konrad Steffen for GC-Net data.

20

Greenland surface water

N. S. Arnold et al.

[Title Page](#)[Abstract](#)[Introduction](#)[Conclusions](#)[References](#)[Tables](#)[Figures](#)[|◀](#)[▶|](#)[Back](#)[Close](#)[Full Screen / Esc](#)[Printer-friendly Version](#)[Interactive Discussion](#)

References

- Arnold, N. S.: A new approach for dealing with depressions in digital elevation models when calculating flow accumulation values, *Prog. Phys. Geog.*, 34, 781–809, doi:10.1177/0309133310384542, 2010.
- 5 Arnold, N., Richards, K., Willis, I., and Sharp, M.: Initial results from a distributed, physically based model of glacier hydrology, *Hydrol. Process.*, 12, 191–219, doi:10.1002/(SICI)1099-1085(199802)12:2<191::AID-HYP571>3.0.CO;2-C, 1998.
- 10 Banwell, A. F., Willis, I. C., Arnold, N. S., Messerli, A., Rye, C. J., and Ahlstrøm, A. P.: Calibration and validation of a high resolution surface mass balance model for Paakitsoq, West Greenland, *J. Glaciol.*, 58, 1047–1062, doi:10.3189/2012JoG12J034, 2012a.
- 15 Banwell, A. F., Arnold, N. S., Willis, I. C., Tedesco, M., and Ahlstrom, A. P.: Modelling supraglacial water routing and lake filling on the Greenland Ice Sheet, *J. Geophys. Res.-Earth*, 117, F04012, doi:10.1029/2012JF002393, 2012b.
- Banwell, A. F., Willis, I. C., and Arnold, N. S.: Modeling subglacial water routing at Paakitsoq, W Greenland, *J. Geophys. Res.-Earth*, 118, 1282–1295, doi:10.1002/jgrf.20093, 2013.
- 20 Banwell, A. F., Caballero, M., Arnold, N. S., Glasser, N. F., Cathles, L. M., and MacAyeal, D. R.: Supraglacial lakes on the Larsen B Ice Shelf, Antarctica, and the Paakitsoq Region, Greenland: A comparative study, *Ann. Glaciol.*, 55, doi:10.3189/2014AoG66A049, 2014.
- Bartholomew, I., Nienow, P., Mair, D., Hubbard, A., King, M. A., and Sole, A.: Seasonal evolution of subglacial drainage and acceleration in a Greenland outlet glacier, *Nat. Geosci.*, 3, 408–411, 2010.
- 25 Bartholomew, I., Nienow, P., Sole, A., Mair, D., Cowton, T., Palmer, S., and King, M.: Seasonal variations in Greenland Ice Sheet motion: Inland extent and behaviour at higher elevations, *Earth Planet. Sc. Lett.*, 307, 271–278, doi:10.1016/j.epsl.2011.04.014, 2011.
- Bartholomew, I., Nienow, P., Sole, A., Mair, D., Cowton, T., and King, M.: Short-term variability in Greenland Ice Sheet motion forced by time-varying meltwater drainage: implications for the relationship between subglacial drainage system behavior and ice velocity, *J. Geophys. Res.-Earth*, 117, F03002, doi:10.1029/2011JF002220, 2012.
- 30 Box, J. E. and Ski, K.: Remote sounding of Greenland supra-glacial melt lakes: implications for subglacial hydraulics, *J. Glaciol.*, 53, 257–264, 2007.

TCD

7, 6143–6170, 2013

Greenland surface water

N. S. Arnold et al.

[Title Page](#)

[Abstract](#)

[Introduction](#)

[Conclusions](#)

[References](#)

[Tables](#)

[Figures](#)

◀

▶

[Back](#)

[Close](#)

[Full Screen / Esc](#)

[Printer-friendly Version](#)

[Interactive Discussion](#)



[Title Page](#)[Abstract](#)[Introduction](#)[Conclusions](#)[References](#)[Tables](#)[Figures](#)[|◀](#)[▶|](#)[◀](#)[▶](#)[Back](#)[Close](#)[Full Screen / Esc](#)[Printer-friendly Version](#)[Interactive Discussion](#)

Chander, G., Markham, B. L., and Helder, D. L.:Summary of current radiometric calibration coefficients for Landsat MSS, TM, ETM+, and EO-1 ALI sensors, *Remote Sens. Environ.*, 113, 893–903, doi:10.1016/j.rse.2009.01.007, 2009.

Clason, C., Mair, D. W. F., Burgess, D. O., and Nienow, P. W.: Modelling the delivery of supraglacial meltwater to the ice/bed interface: application to Southwest Devon Ice Cap, Nunavut, Canada, *J. Glaciol.*, 58, 361–374, doi:10.3189/2012JoG11J129, 2012.

Cowton, T., Nienow, P., Sole, A., Wadham, J., Lis, G., Bartholomew, I., Mair, D., and Chandler, D.: Evolution of drainage system morphology at a land-terminating Greenlandic outlet glacier, *J. Geophys. Res.-Earth*, 118, 29–41, doi:10.1029/2012JF002540, 2013.

Das, S., Joughin, M., Behn, M., Howat, I., King, M., Lizarralde, D., Bhatia, M. P.: Fracture propagation to the base of the Greenland Ice Sheet during supra-glacial lake drainage, *Science*, 320, 778–781, 2008.

DiMarzio, J., Brenner, A., Schutz, R., Shuman, C. A., and Zwally, H. J.: GLAS/ICESat 1 km laser altimetry digital elevation model of Greenland, National Snow and Ice Data Center, Boulder, Colorado USA, digital media, 2007.

Echelmeyer, K., Clarke, T. S., and Harrison, W. D.: Surficial glaciology of Jakobshavn Isbræ, West Greenland: Part I. Surface morphology, *J. Glaciol.*, 37, 368–382, 1991.

Fitzpatrick, A. A. W., Hubbard, A. L., Box, J. E., Quincey, D. J., van As, D., Mikkelsen, A. P. B., Doyle, S. H., Dow, C. F., Hasholt, B., and Jones, G. A.: A decade of supraglacial lake volume estimates across a land-terminating margin of the Greenland Ice Sheet, *The Cryosphere Discuss.*, 7, 1383–1414, doi:10.5194/tcd-7-1383-2013, 2013.

Hoffman, M. J., Catania, G. A., Neumann, T. A., Andrews, L. C., and Rumrill, J. A.: Links between acceleration, melting, and supraglacial lake drainage of the western Greenland Ice Sheet, *J. Geophys. Res.-Earth*, 116, F04035, doi:10.1029/2010JF001934, 2011.

Howat, I. M., Negrete, A., Scambos, T., Haran, T.: A high-resolution elevation model for the Greenland Ice Sheet from combined stereoscopic and photoclinometric data, in preparation, <http://bprc.osu.edu/GDG/gimpdem.php> (last access: 19 December 2013), 2012.

Joughin, I., Das, S. B., Flowers, G. E., Behn, M. D., Alley, R. B., King, M. A., Smith, B. E., Bamber, J. L., van den Broeke, M. R., and van Angelen, J. H.: Influence of ice-sheet geometry and supraglacial lakes on seasonal ice-flow variability, *The Cryosphere*, 7, 1185–1192, doi:10.5194/tc-7-1185-2013, 2013.

Krause, P., Boyle, D. P., and Bäse, F.: Comparison of different efficiency criteria for hydrological model assessment, *Adv. Geosci.*, 5, 89–97, doi:10.5194/adgeo-5-89-2005, 2005.

- Liang, Y., Colgan, W., Lv, Q., Steffen, K., Abdalaiti, W., Stroeve, J., Gallaher, D., and Bayou, N.: A decadal investigation of supraglacial lakes in West Greenland using a fully automatic detection and tracking algorithm, *Remote Sens. Environ.*, 123, 127–138, 2012.
- Luthje, M., Pedersen, L. T., Reeh, N., and Greuell, W.: Modelling the evolution of supra-glacial lakes on the West Greenland Ice Sheet margin, *J. Glaciol.*, 52, 608–618, 2006.
- McMillan, M., Nienow, P., Shepherd, A., Benham, T., and Sole, A.: Seasonal evolution of supra-glacial lakes on the Greenland Ice Sheet, *Earth Planet. Sc. Lett.*, 262, 484–492, 2007.
- Morriss, B. F., Hawley, R. L., Chipman, J. W., Andrews, L. C., Catania, G. A., Hoffman, M. J., Lüthi, M. P., and Neumann, T. A.: A ten-year record of supraglacial lake evolution and rapid drainage in West Greenland using an automated processing algorithm for multispectral imagery, *The Cryosphere Discuss.*, 7, 3543–3565, doi:10.5194/tcd-7-3543-2013, 2013.
- Rye, C. J., Arnold, N. S., Willis, I., and Kohler, J.: Modelling the surface mass balance of a High Arctic glacier using the ERA-40 Reanalysis, *J. Geophys. Res.-Earth*, 115, F02014, doi:10.1029/2009JF001364, 2010.
- Schoof, C.: Ice-sheet acceleration driven by melt supply variability, *Nature*, 468, 803–806, doi:10.1038/nature09618, 2010.
- Selmes, N., Murray, T., and James, T. D.: Fast draining lakes on the Greenland Ice Sheet, *Geophys. Res. Lett.*, 38, L15501, doi:10.1029/2011GL047872, 2011.
- Sneed, W. A. and Hamilton, G. S.: Evolution of melt pond volume on the surface of the Greenland Ice Sheet, *Geophys. Res. Lett.*, 34, L03501, doi:10.1029/2006GL028697, 2007.
- Sole, A. J., Mair, D. W. F., Nienow, P. W., Bartholomew, I. D., King, M. A., Burke, M. J., and Joughin, I.: Seasonal speedup of a greenland marine-terminating outlet glacier forced by surface melt induced changes in subglacial hydrology, *J. Geophys. Res.*, 116, F03014, doi:10.1029/2010jf001948, 2011.
- Sole, A., Nienow, P., Bartholomew, I., Mair, D., Cowton, T., Tedstone, A., and King, M. A.: Winter motion mediates dynamic response of the Greenland Ice Sheet to warmer summers, *Geophys. Res. Lett.*, 40, 3940–3944, doi:10.1002/grl.50764, 2013.
- Sundal, A. V., Shepherd, A., Nienow, P., Hanna, E., Palmer, S., and Huybrechts, P.: Evolution of supra-glacial lakes across the Greenland Ice Sheet, *Remote Sens. Environ.*, 113, 2164–2171, 2009.
- Sundal, A. V., Shepherd, A., Nienow, P., Hanna, E., Palmer, S., and Huybrechts, P.: Melt-induced speed-up of Greenland ice sheet offset by efficient subglacial drainage, *Nature*, 469, 522–523, doi:10.1038/nature09740, 2011.

[Title Page](#)[Abstract](#)[Introduction](#)[Conclusions](#)[References](#)[Tables](#)[Figures](#)[◀](#)[▶](#)[◀](#)[▶](#)[Back](#)[Close](#)[Full Screen / Esc](#)[Printer-friendly Version](#)[Interactive Discussion](#)

Tedesco, M., Willis, I., Hoffman, M., Banwell, A. F., Alexander, P., and Arnold, N.: Ice dynamic response to two modes of surface lake drainage on the Greenland Ice Sheet, Environ. Res. Lett., 8, 034007, doi:10.1088/1748-9326/8/3/034007, 2013.

Van der Veen, C. J.: Fracture Propagation as means of rapidly transferring surface meltwater to the base of glaciers, Geophys. Res. Lett., 34, L01501, doi:10.1029/2006GL028385, 2007.

Zwally, H. J., Abdalati, W., Herring, T., Larson, K., Saba, J., and Steffen, K.: Surface melt-induced acceleration of Greenland ice-sheet flow, Science, 297, 218–222, 2002.

TCD

7, 6143–6170, 2013

Greenland surface water

N. S. Arnold et al.

[Title Page](#)

[Abstract](#)

[Introduction](#)

[Conclusions](#)

[References](#)

[Tables](#)

[Figures](#)

[|◀](#)

[▶|](#)

[◀](#)

[▶](#)

[Back](#)

[Close](#)

[Full Screen / Esc](#)

[Printer-friendly Version](#)

[Interactive Discussion](#)



Table 1. Co-location statistics for observed lakes and DEM depressions.

Band1/ Band3 Threshold	Number of separate lakes (n)	Number of lake centroids in DEM depressions (A)	Additional number of centroids within 2 pixels	Mean number of randomly distributed centroids in depressions (for 1000 sets)	Standard deviation of number of randomly distributed centroids in depressions	z score of A
2	505	252	74	39.4	6.0	42
3	229	179	0	14.8	3.6	49.7

Title Page

Abstract

Introduction

Conclusions

References

Tables

Figures

|◀

▶|

◀

▶

Back

Close

Full Screen / Esc

Printer-friendly Version

Interactive Discussion



[Title Page](#)[Abstract](#)[Introduction](#)[Conclusions](#)[References](#)[Tables](#)[Figures](#)[|◀](#)[▶|](#)[◀](#)[▶](#)[Back](#)[Close](#)[Full Screen / Esc](#)[Printer-friendly Version](#)[Interactive Discussion](#)**Table 2.** Model performance for different fracture area thresholds (F_a , m²).

Year (No. of images)	F_a	R^2	Slope	wR ² ^a	Nash
2001 (4)	1000	0.881	0.590	0.520	0.749
	2500	0.894	0.545	0.487	0.741
	4000	0.889	0.676	0.601	0.828
	5000	0.819	0.736	0.603	0.807
	7500	0.805	0.792	0.638	0.805
	10 000	0.804	0.867	0.697	0.799
	Inf. ^b	0.717	1.336	0.537	0.155
2002 (4)	1000	0.603	0.361	0.218	0.460
	2500	0.741	0.615	0.456	0.697
	4000	0.851	0.854	0.726	0.843
	5000	0.849	0.905	0.768	0.840
	7500	0.845	0.902	0.762	0.838
	10 000	0.928	1.224	0.758	0.833
	Inf.	0.907	1.527	0.594	0.471
2005 (1)	1000	0.679	0.564	0.832	0.62
	2500	0.750	0.651	0.489	0.716
	4000-Inf.	As 2500			

^a Weighted R^2 ; see Sect. 2.4.^b No drainage events allowed.

Greenland surface water

N. S. Arnold et al.

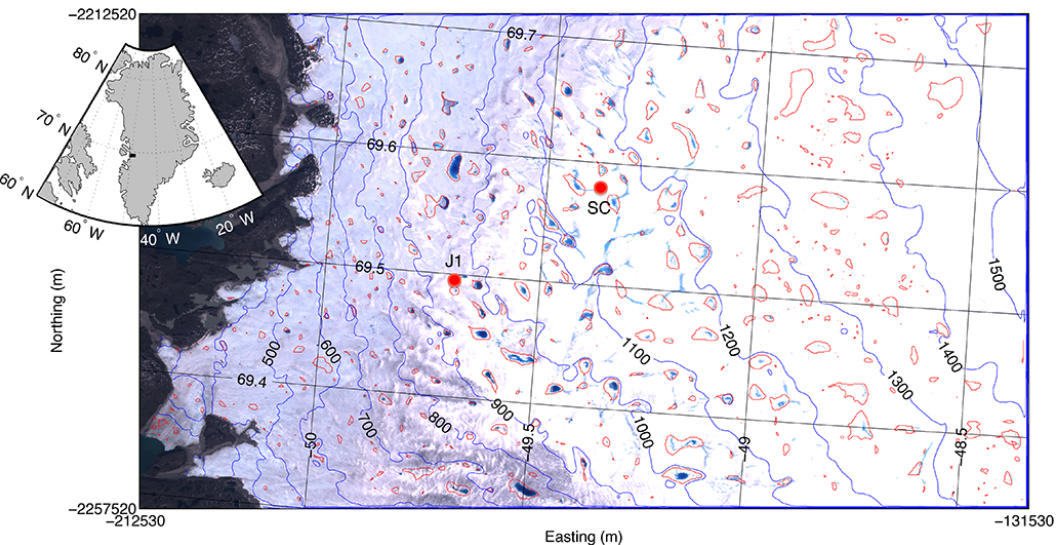


Fig. 1. Location map of the study area. Detailed map shows Landsat true-colour image for 7 July 2001. Red lines show maximum possible lake extents calculated from the DEM using the method of Arnold (2010). Black rectangle in inset map shows study area location within Greenland. Red circles show locations of JAR-1 (J1) and Swiss Camp (SC) GC-Net stations.

[Title Page](#)[Abstract](#)[Introduction](#)[Conclusions](#)[References](#)[Tables](#)[Figures](#)[|◀](#)[▶|](#)[◀](#)[▶](#)[Back](#)[Close](#)[Full Screen / Esc](#)[Printer-friendly Version](#)[Interactive Discussion](#)

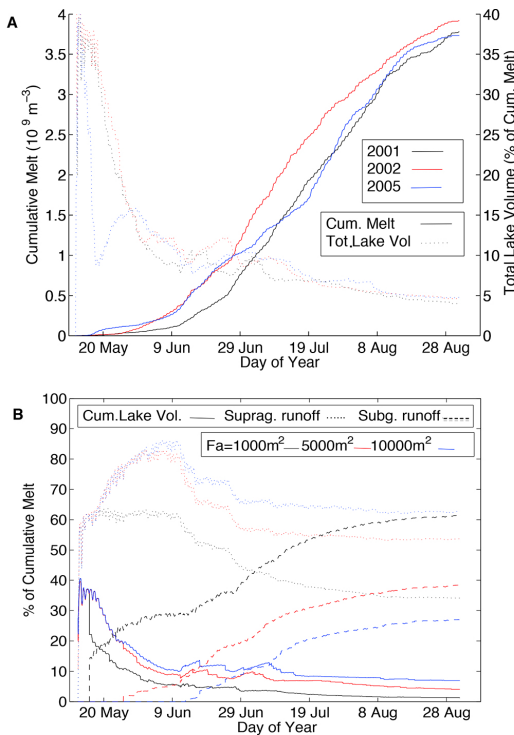


Fig. 2. (a) Modelled evolution of total water storage (as a proportion of total meltwater production) in lakes in comparison with total modelled meltwater for the three years discussed in the text, for $F_a = 5000 \text{ m}^2$. **(b)** Cumulative lake volume (Cum. Lake Vol.), the cumulative amount of melt which runs off the surface of the ice sheet (Suprag. runoff), and the cumulative amount of melt which enters the subglacial drainage system via drained lakes (Subg. runoff), all as proportions of total cumulative melt for 2001, for $F_a = 1000 \text{ m}^2$; 5000 m^2 and $10\,000 \text{ m}^2$.

[Title Page](#) | [Abstract](#) | [Introduction](#)
[Conclusions](#) | [References](#)
[Tables](#) | [Figures](#)
[◀](#) | [▶](#)
[◀](#) | [▶](#)
[Back](#) | [Close](#)
[Full Screen / Esc](#)

[Printer-friendly Version](#)
[Interactive Discussion](#)



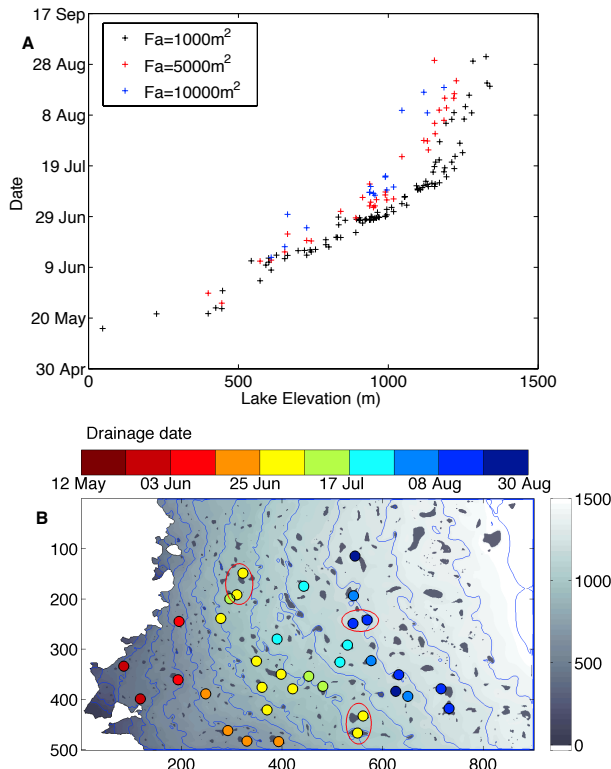


Fig. 3. (a) Up-ice sheet progression of lake drainage events during 2001 for $F_a = 1000 \text{ m}^2$ (black) 5000 m^2 (red) and 10000 m^2 (blue). (b) Spatial distribution of drainage events during 2001 for $F_a = 5000 \text{ m}^2$. Adjacent lakes that drain within 24 h are highlighted with red ellipses.

[Title Page](#)[Abstract](#)[Introduction](#)[Conclusions](#)[References](#)[Tables](#)[Figures](#)[|◀](#)[▶|](#)[◀](#)[▶](#)[Back](#)[Close](#)[Full Screen / Esc](#)[Printer-friendly Version](#)[Interactive Discussion](#)

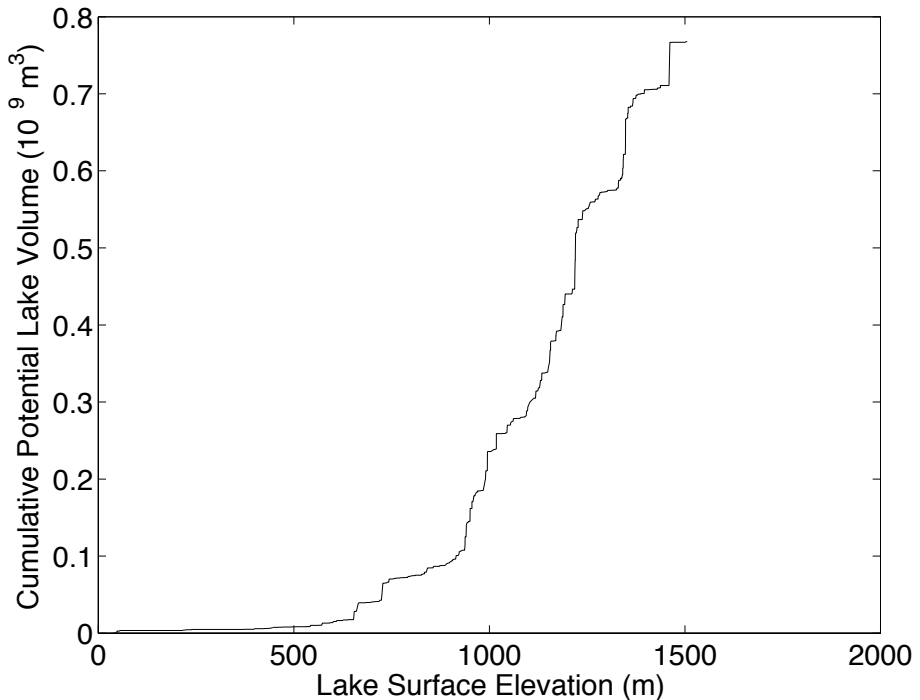


Fig. 4. Cumulative maximum potential surface water storage in surface depressions by elevation for the Paakitsoq region.